Random sequential adsorption of polydisperse mixtures on discrete substrates

Lj. Budinski-Petković,[1] S. B. Vrhovac,[2,*] and I. Lončarević[1]

[1]*Faculty of Engineering, Trg D. Obradovića 6, 21000 Novi Sad, Serbia*
[2]*Institute of Physics, P.O. Box 68, 11080 Zemun, Belgrade, Serbia*

We study random sequential adsorption of polydisperse mixtures of extended objects both on a triangular and on a square lattice. The depositing objects are formed by self-avoiding random walks on two-dimensional lattices. Numerical simulations were performed to determine the influence of the number of mixture components and length of the shapes making the mixture on the kinetics of the deposition process. We find that the late stage deposition kinetics follows an exponential law $\theta(t) \sim \theta_{jam} - A \exp(-t/\sigma)$ not only for the whole mixture, but also for the individual components. We discuss in detail how the quantities such as jamming coverage θ_{jam} and the relaxation time σ depend on the mixture composition. Our results suggest that the order of symmetry axis of the shape may exert a decisive influence on adsorption kinetics of each mixture component.

I. INTRODUCTION

Random sequential adsorption (RSA) is a classical model of irreversible adsorption on substrates. A number of processes in physics, chemistry, and biology, where the microscopic events occur essentially irreversibly on the time scales of the experiment, can be studied as random sequential adsorption on a lattice. For example, the adsorption of large particles such as colloids, proteins, or latexes on substrates is often a highly irreversible process.

Random sequential adsorption, or irreversible deposition, is a process in which the objects of a specified shape are randomly and sequentially deposited onto a substrate. We shall focus our attention on the monolayer deposition where depositing objects are not allowed to overlap. The adsorbed particles are permanently fixed at their spatial positions. Once an object is placed it affects the geometry of all later placements, so the dominant effect in RSA is the blocking of the available substrate area. The deposition process ceases when all unoccupied spaces are smaller than the size of an adsorbed particle. The system is then jammed in a nonequilibrium disordered state for which the limiting (jamming) coverage θ_{jam} is less than the corresponding density of closest packing. The kinetic properties of a deposition process are described by the time evolution of the coverage $\theta(t)$, which is the fraction of the substrate area occupied by the adsorbed particles. For a review of RSA models see Refs. [1–4].

Exact solutions for RSA models are available for only two limiting cases: deposition of k-mer particles on the linear lattice in one dimension [5–7] and quasi-one-dimensional systems [8,9]. The placing of an object on a line divides the line into two independent systems that can be treated separately. This is an essential property that has made analytic progress possible and it does not exist for two-dimensional lattices. Two-dimensional problems are most likely intractable and Monte Carlo simulations remain one of the primary

tools for investigating deposition problems [10–15].

The most interesting property of the RSA process is the time dependence of the approach to the jammed state at large times. Depending on the system of interest modeled by RSA, substrate can be continuum or discrete. Approach to the jamming coverage is known to be asymptotically algebraic for continuum systems [16–19] and exponential for lattice models [10,11,20–22]. For the latter case the approach of the coverage fraction to its jamming limit is given by the time dependence

$$\theta(t) = \theta_{jam} - A e^{-t/\sigma}, \tag{1}$$

where A and σ are parameters that depend on the shape, on the orientational freedom of the objects, on the type of depositing particles—monodisperse or mixtures, etc.

There are numerous studies concerning the role of polydispersity in irreversible deposition. Examples include binary mixtures [23–25] and mixtures of particles obeying various (uniform, Gaussian, power-law) size distributions [24,26,27]. The deposition of two-component mixtures of line segments on a square lattice is discussed in Ref. [28]. It is concluded by numerical simulations that the mixtures cover the lattice more efficiently than either of the species separately. Theoretical works were restricted only to binary mixtures of particles with very large size differences [6,29,30] and mixtures with power-law size distribution of particles [27,31]. However, very little attention has been given to the similar monolayer growth by more than two species of different shape and/or size [11,22], despite the fact that the polydisperse case is much closer to many real physical situations. In this paper we focus our attention on the RSA of polydisperse mixtures containing depositing objects of various shapes and sizes.

The results are obtained by Monte Carlo simulations. The depositing objects are made by directed self-avoiding random walks on a two-dimensional (2D) triangular lattice. On a triangular lattice objects with a symmetry axis of first, second, third, and sixth order can be formed. Rotational symmetry of order n_s, also called n_s-fold rotational symmetry, with respect to a particular axis perpendicular to the triangular lattice, means that rotation by an angle of $2\pi/n_s$ does not

TABLE I. The partial jamming coverages θ_{jam} and the relaxation times σ for the line segments of length l making a ten-component mixture as well as the total jamming coverage and the relaxation time for the mixture.

Shape		θ_{jam}	σ
●—●	$l=1$	0.2960(3)	30.1(7)
●—●—●	$l=2$	0.1505(4)	9.78(20)
…	$l=3$	0.1041(2)	5.05(10)
…	$l=4$	0.0799(3)	2.62(7)
…	$l=5$	0.0665(4)	1.43(4)
…	$l=6$	0.0580(4)	1.04(4)
…	$l=7$	0.0509(3)	0.84(3)
…	$l=8$	0.0467(3)	0.62(2)
…	$l=9$	0.0427(4)	0.41(1)
…	$l=10$	0.0397(3)	0.30(1)
Mixture		0.9350(1)	30.1(7)

TABLE II. The partial jamming coverages θ_{jam} and the relaxation times σ for the ten-component mixture of the angled objects of size s, as well as the total jamming coverage and the relaxation time for the mixture. Larger objects are made by repeating each step of the basic object corresponding number of times.

Shape		θ_{jam}	σ
●—● /	$s=1.5$	0.3888(3)	57.3(9)
●—●—● /	$s=3$	0.1343(4)	26.1(7)
…	$s=4.5$	0.0771(3)	15.8(4)
…	$s=6$	0.0532(3)	10.9(3)
…	$s=7.5$	0.0408(4)	8.55(20)
…	$s=9$	0.0330(4)	7.37(15)
…	$s=10.5$	0.0291(4)	6.32(15)
…	$s=12$	0.0254(4)	5.07(10)
…	$s=13.5$	0.0230(5)	4.04(10)
…	$s=15$	0.0207(2)	3.27(10)
Mixture		0.8255(3)	57.3(9)

change the object. For RSA of monodisperse particles [11] and for the deposition of two-component mixtures [14] it has been shown that the kinetics of the process depends mainly on the symmetry properties of the objects.

In the case of polydisperse mixtures we investigate the dependence of the deposition kinetics on the number of components in the mixture and on the length of the walks making the mixture, the influence of the symmetry properties of depositing objects, and we give the results not only for the whole mixture, but also for the individual components. In this paper we also report the results of numerical simulations concerning adsorption of polydisperse mixtures of extended objects on a square lattice. Section II describes the details of the simulations. We give the simulation results and discussions in Sec. III. Finally, Sec. IV contains some additional comments and final remarks.

II. DEFINITION OF THE MODEL AND THE SIMULATION METHOD

The polydisperse mixtures of extended objects on a two-dimensional triangular lattice used in our simulations are shown in Tables I–IV. Linear segments (k-mers) and angled objects that constitute the ten-component mixtures of objects of various sizes are presented in Tables I and II, respectively. Triangles that constitute the five-component mixture are shown in Table III. In Table IV three different shapes that can be made by the self-avoiding walks of length $l=2$ are shown. It should be noted that the size s of an object is taken as the greatest projection of the walk that makes the object on one of the six directions. Thus the size of a dot is $s=0$, the size of a one-step walk is $s=1$, and for example, the size of the first object in Table II is $s=1.5$ in lattice spacing.

The Monte Carlo simulations are performed on a 2D triangular lattice of size $L=128$. Periodic boundary conditions are used in all directions. The finite-size effects, which are generally weak, can be neglected for object sizes $<L/8$ [10].

At each Monte Carlo step a lattice site is selected at random and one of the objects making the mixture is selected at

random. If the selected site is unoccupied deposition of the selected object is tried in one of the six orientations. We fix the beginning of the walk that makes the shape at the selected site and search whether all successive l sites are unoccupied. If so, we occupy these $l+1$ sites and place the object. If the attempt fails, a new site and a new depositing object from the mixture are selected at random. The jamming limit is reached when neither of the objects can be placed in any position on the lattice. This scheme is usually called conventional or standard model of RSA. The other strategy to perform an RSA, where we check all possible directions from the selected site, is named the end-on model [11].

Simulations were also performed for mixtures of self-avoiding random walk chains of various lengths on a square lattice of size $L=128$. Chains are modeled by self-avoiding random walks of length l on a square lattice. A chain of length l is a sequence of distinct vertices $(\omega_0, \dots, \omega_l)$ such that each vertex is a nearest neighbor of its predecessor, i.e., a chain of length l covers $l+1$ lattice sites. In the case of an

TABLE III. The partial jamming coverages θ_{jam} and the relaxation times σ for the triangles of size s making a five-component mixture as well as the total jamming coverage and the relaxation time for the mixture. Each object occupies all comprised sites on lattice.

Shape		θ_{jam}	σ
◺	$s=1$	0.3358(6)	9.80(15)
◿	$s=2$	0.1635(4)	1.74(5)
…	$s=3$	0.1260(5)	0.664(10)
…	$s=4$	0.1131(8)	0.230(6)
…	$s=5$	0.1108(7)	0.119(4)
Mixture		0.8492(2)	9.80(15)

TABLE IV. The partial and the total jamming coverages θ_{jam} and the relaxation times σ for the three-component mixture of various objects of different rotational symmetries n_s, but of the same number of segments $\ell = 2$.

Shape		θ_{jam}	σ
•—•—•	$n_s = 2$	0.2877(3)	8.40(20)
⌐	$n_s = 1$	0.2958(5)	18.1(4)
⌐	$n_s = 3$	0.2935(5)	6.15(10)
Mixture		0.8770(2)	17.9(4)

n-component mixture, n chains of fixed length l are made at the beginning of each independent simulation. These chains are deposited onto the lattice with equal probability. At each deposition attempt one of the chains is selected at random, a lattice site is selected at random and deposition of the chain is tried in one of the four possible orientations. The jamming limit for a specified mixture is reached when neither of the chains making the mixture can be deposited in any position.

In all the simulations the time is counted by the number of attempts to select a lattice site and scaled by the total number of lattice sites. The data is averaged over 1000 independent runs for each mixture of depositing objects.

III. RESULTS AND DISCUSSION

Example results for the time dependence of $\ln[\theta_{\text{jam}} - \theta(t)]$ are shown in Fig. 1, both for the five-component mixture of line segments of lengths $l = 1, 2, \ldots, 5$ from Table I and for the five-component mixture of triangles of various sizes $s = 1, 2, \ldots, 5$ from Table III. We can see that for the late stages of the process these plots are straight lines not only for the mixtures, but also for each of the components. Similar results are obtained for the deposition of mixture of angled objects from Table II. This suggests that the approach to the jamming limit is exponential of the form (1) both for the mixture and for the components making the mixture.

The values of the partial jamming coverages θ_{jam} for the components making the ten-component mixture of line segments of lengths $l = 1, 2, \ldots, 10$ are given in Table I, together with the total jamming coverage for the mixture. The results for the partial and total jamming coverages for the ten-component mixture of angled objects are given in Table II, and the results for the five-component mixture of triangles are given in Table III. The values of the parameter σ are determined from the slopes of the plots of $\ln[\theta_{\text{jam}} - \theta(t)]$ vs t and they are given in the last column of each table. Parameter σ determines how fast the lattice is filled up to the jamming coverage θ_{jam}. All these results are also shown in Figs. 2 and 3. In Tables I–IV, the numbers in parentheses are the numerical values of the standard uncertainty of θ_{jam} and σ referred to the last digits of the quoted value.

From Fig. 2 we can see that the partial jamming coverages decrease very rapidly with the size of the objects. Noticeable drop in the partial coverage fraction is thus a clear consequence of the enhanced frustration of the spatial ad-
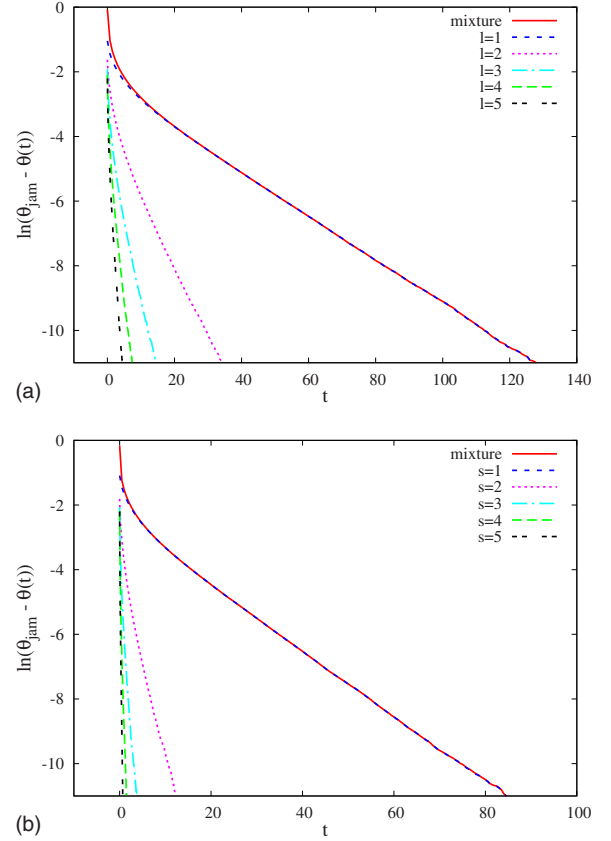

FIG. 1. (Color online) Plots of $\ln[\theta_{\text{jam}} - \theta(t)]$ vs t for the five-component mixture of (a) line segments of lengths $l = 1, 2, \ldots, 5$ (Table I) and (b) triangles of various sizes $s = 1, 2, \ldots, 5$ (Table III).

sorption. At the beginning of the deposition process, when the lattice is empty, the largest objects are deposited with equal adsorption rate as the smallest ones. However, when the lattice is partially filled with objects of various sizes, it is much easier to place the smaller objects at random so that the adsorption of large objects is suppressed. Moreover, the decrease of the partial jamming coverage with the size of the objects is faster for the mixtures of asymmetric objects than for the mixtures of more regular and symmetric shapes. Indeed, if one examines the snapshots of patterns formed during the deposition process, it can be observed that the growth of domains precipitated during the early growth is very efficient for the cases of line segments and triangles but is frustrated in the case of angled objects. The sizes of these domains have significant influence on the kinetics of RSA in the late phase of adsorption, resulting in smaller values of the partial jamming coverage fraction in the case of less symmetric objects.

Moreover, the values of the parameter σ are generally greater for the mixtures of less symmetric objects (see Fig. 3). This is in agreement with the results for monodisperse deposition [11,14] according to which the rapidity of the approach to the jamming limit is slower for less symmetric objects. The symmetry properties of the shapes have an essential influence in the late times of the deposition process. Namely, a shape with a symmetry axis of higher order has a greater number of possible orientations for deposition into
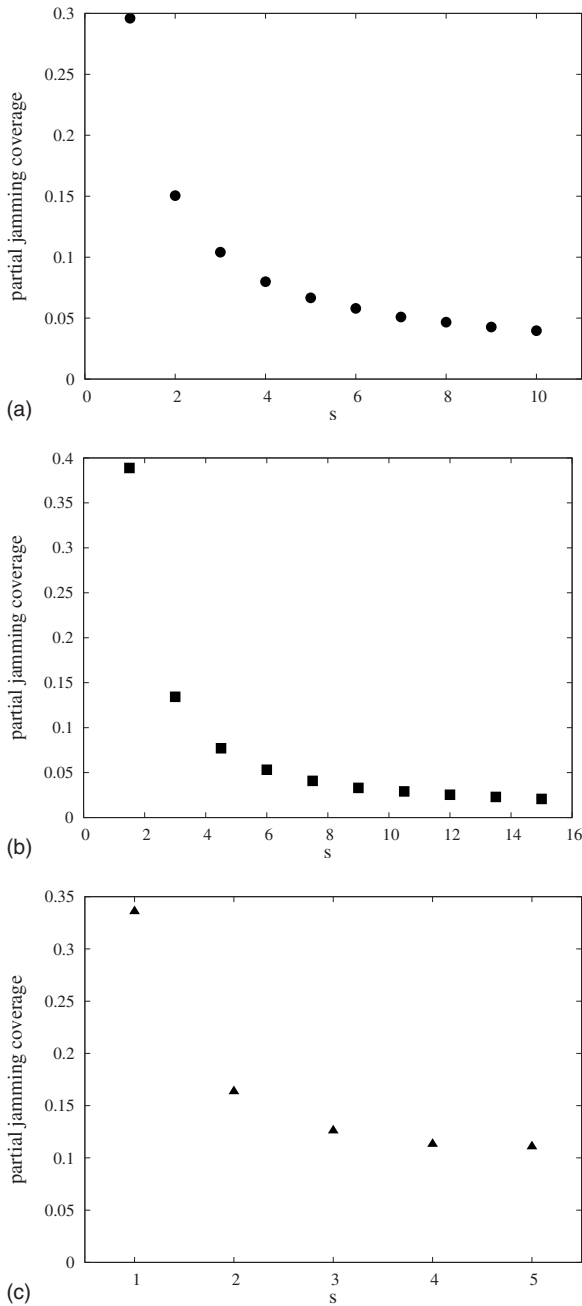
FIG. 2. Dependence of the partial jamming coverages θ_{jam} on the size s of the objects for (a) ten-component mixture of line segments (Table I), (b) ten-component mixture of angled objects (Table II), and (c) five-component mixture of triangles (Table III). For θ_{jam} the error bars are smaller than the symbol size.

FIG. 3. Dependence of the parameter σ on the size s of the objects for the ten-component mixture of angled objects (Table II), the ten-component mixture of line segments (Table I), and the five-component mixture of triangles (Table III). For σ the error bars are smaller than the symbol size.

small isolated locations on the lattice and, therefore, an enhanced probability for deposition. The relaxation time σ decreases rapidly with the size of the component making the mixture, so that in the late times the kinetics of the deposition is determined mostly by the smallest objects in the mixture. The reasons for these results are intuitively clear. Due to the fact that the densification kinetics is dictated by geometric exclusion effects, in the competition for the deposition between two objects of different number of segments the smaller shape wins.
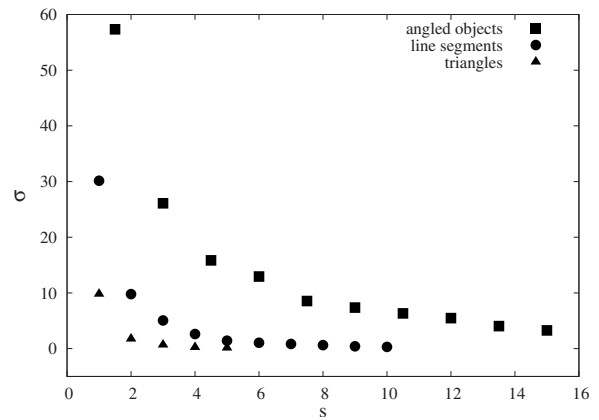
Dependence of the kinetics of the deposition process on the number of components in the mixture is also studied. The results for the jamming coverage θ_{jam} are shown for the mixture of line segments in Fig. 4(a), for the angled objects in Fig. 4(b), and for the triangles in Fig. 4(c). For example, the two-component mixture of line segments consists of the lines of length $l=1$ and $l=2$, the three-component mixture is made by adding a line segment of length $l=3$, and so on. An n-component mixture contains lines of length $l=1,2,\ldots,n$, and all of them are adsorbed with equal probability. Mixtures of the other two shapes, i.e., angled objects and triangles, are made in a similar way.

As can be seen from Fig. 4, larger values of the total jamming coverage fraction are reached by the deposition process involving the line segments (k-mers) compared to a similar process involving the angled objects. The pattern formed during the deposition is made up of a large number of domains. In the case of the deposition of line segments, any such domain contains a large number of objects all close to each other and parallel. However, the growth of domains is substantially frustrated in the case of the angled objects. This is reflected in the relatively low local packing of adsorbed objects in the vicinity of a given object in the case of the angled objects, as compared to the more symmetric line segments, resulting in a smaller value of the jamming coverage fraction in the former case.

Figure 4 also shows that for the line segments and for the triangles jamming coverages increase with n, in spite of the fact that the number of components is always increased by adding an object of a greater size. On the contrary, for the angled objects there is a greater probability for blocking the neighboring sites and the jamming coverage decreases with the number of components in the mixture. For each n, the plots of $\ln[\theta_{\text{jam}} - \theta(t)]$ vs t are straight lines and the values of the parameter σ are obtained from the slopes of these lines. These results are shown in Fig. 5. It is interesting that the relaxation time σ grows linearly with the number of components in the mixture. As expected, this growth is slower for more symmetric objects.
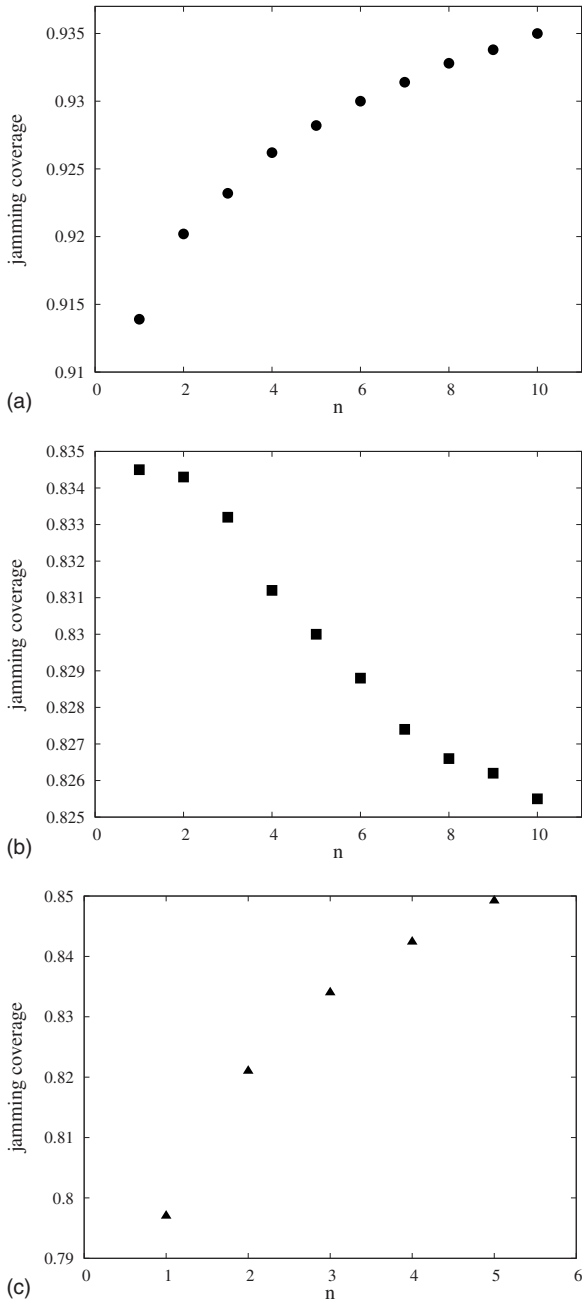
(a)

(b)

(c)

FIG. 4. Dependence of the jamming coverage θ_{jam} on the number of components in the mixture for the mixtures of (a) line segments, (b) angled objects, (c) triangles. The number of components n is always increased by adding an object of a greater size. Here the error bars do not exceed the size of the symbols.

A three-component mixture of various shapes is shown in Table IV. These shapes are made by self-avoiding walks of the same length $l=2$, but they differ in their symmetry properties. Plots of $\ln[\theta_{jam}-\theta(t)]$ vs t for these objects are shown in Fig. 6. The corresponding values of the partial and total jamming coverages θ_{jam} and the values of the parameter σ are given in Table IV. The presented results suggest that at late enough times, when the coverage fraction is sufficient to make the geometry of the unoccupied lattice sites complex, the rotational symmetries associated with specific shapes have a substantial influence on the adsorption rate of the
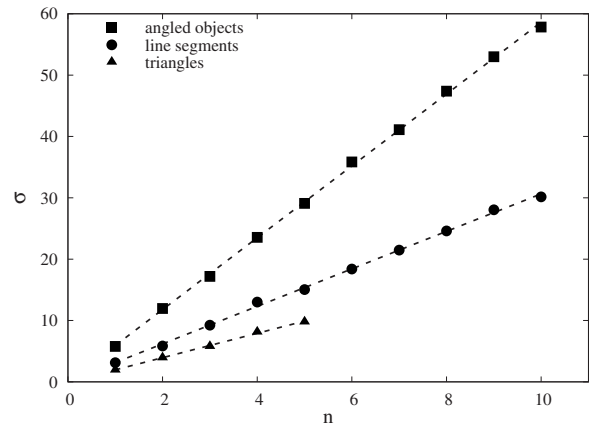

FIG. 5. Dependence of the parameter σ on the number of components in the mixture for the mixtures of angled objects, line segments, and triangles. The number of components n is always increased by adding an object of a greater size. The straight lines are the best linear fits through the data points. The slopes of the corresponding dashed lines are 1.99 ± 0.04, 3.06 ± 0.05, and 5.86 ± 0.05 (from bottom to top lines, respectively). Here the error bars do not exceed the size of the symbols.

mixture components. Indeed, more symmetric objects reach their partial jamming coverage faster, i.e., the relaxation time σ is smaller for more symmetric components in the mixture. Consequently, in the late stage of the process the kinetics of the mixture deposition is determined practically by the deposition of the least symmetric object in the mixture. At large times, adsorption events take place on islands of unoccupied sites. The individual islands act as selective targets for specific deposition events. In other words, there is only a restricted number of possible orientations in which an object can reach a vacant location, provided the location is small enough. For a shape of a higher order of symmetry n_s, there is a greater number of possible orientations for deposition into a selective target on the lattice. Hence, the increase of the order of symmetry of the shape enhances the rate of single particle adsorption. This is reflected in the fact that the adsorption of asymmetric shapes is slower than the adsorption of more regular and symmetric shapes.

Some additional simulations have been performed for mixtures of self-avoiding random walk chains of various
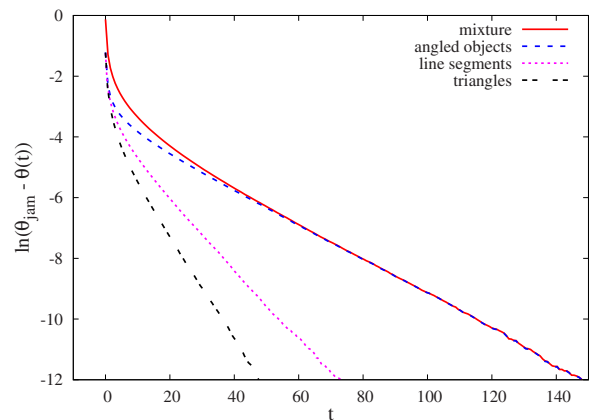

FIG. 6. (Color online) Plots of $\ln[\theta_{jam}-\theta(t)]$ vs t for the three-component mixture shown in Table IV.
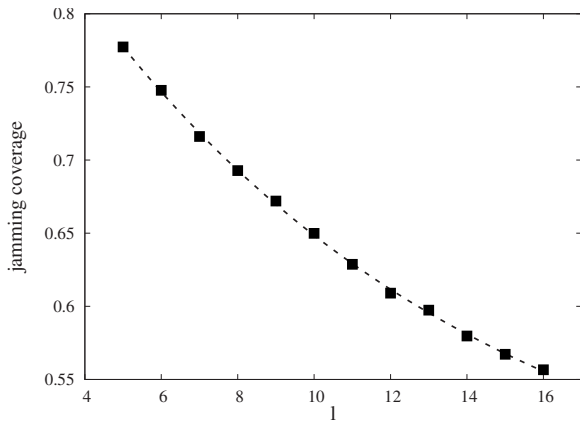
FIG. 7. Dependence of the jamming coverage θ_{jam} on the length l of the chains for a mixture of ten randomly chosen chains on a square lattice. The dashed line represents the exponential fit of the form $\theta_{jam} = \theta_0 + \theta_1 e^{-l/r}$, with $\theta_0 = 0.432 \pm 0.003$, $\theta_1 = 0.551 \pm 0.006$, and $r = 10.73 \pm 0.08$. The statistical error bars do not exceed the size of the symbols.

lengths on a square lattice. At the beginning of each independent run which starts with an empty lattice, a mixture of n randomly made chains was specified. Dependence of the total jamming coverage θ_{jam} on the length of the chains l is shown in Fig. 7 for a ten-component mixture. The jamming coverage θ_{jam} is found to decrease with the chain length l according to an exponential law. The dashed line in Fig. 7 represents the exponential fit of the form

$$\theta_{jam} = \theta_0 + \theta_1 e^{-l/r}, \tag{3}$$

with parameters $\theta_0 = 0.4315$, $\theta_1 = 0.5513$, and $r = 10.73$.

In the case of square lattice, the plots of $\ln[\theta_{jam} - \theta(t)]$ vs t are also straight lines in the late times of the deposition process for all the mixtures. The dependence of the relaxation time σ on the length l of the chains making the ten-component mixture is shown in Fig. 8. As expected, the parameter σ increases with the chain length.
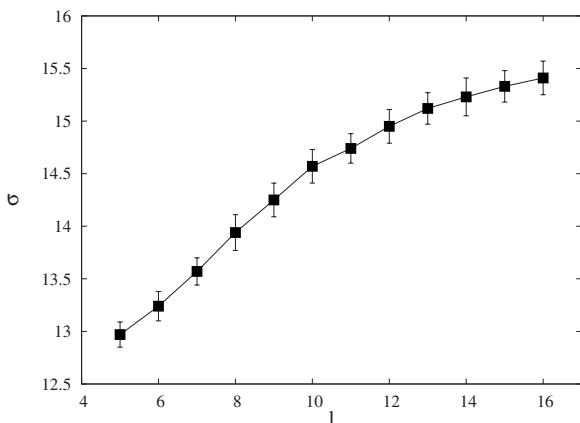

FIG. 8. Dependence of the parameter σ on the length l of the chains for a ten-component mixture of randomly chosen chains on a square lattice. The error bars indicate the standard deviation from the average value.
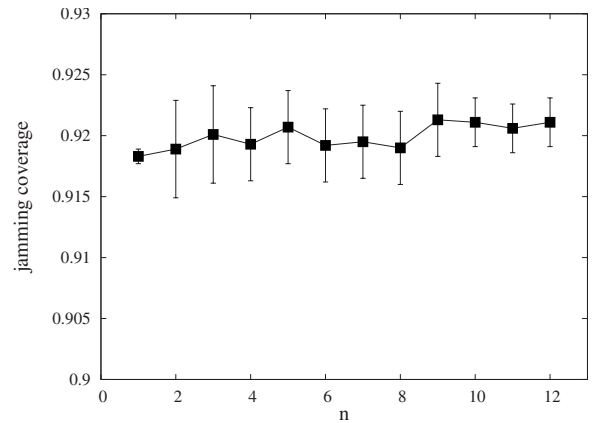

FIG. 9. Dependence of the jamming coverage θ_{jam} on the number of randomly chosen chains in a mixture. The number of components n is always increased by adding a chain made by a walk of a greater length. The error bars indicate the standard deviation from the average value.

Dependence of the jamming coverage θ_{jam} and the dependence of the parameter σ on the number of components making the polydisperse mixture on a square lattice are shown in Figs. 9 and 10, respectively. The number of components n is always increased by adding a chain made by a walk of a greater length, from $n = 1$ and $l = 1$ to $n = 12$ and $l = 1, 2, \ldots, 12$. From Fig. 9, it seems that the jamming coverages fluctuate around ≈ 0.92. We find that the relaxation time σ grows logarithmically with the number of components n, i.e., $\sigma \sim \ln(kn)$.

IV. CONCLUDING REMARKS

We have performed extensive numerical simulations of the irreversible RSA using polydisperse mixtures composed of extended objects on 2D lattices. The role that the polydispersity, size, and the symmetry properties of the shapes play
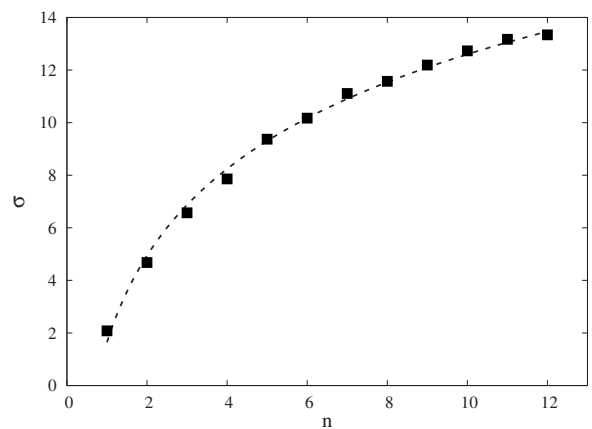

FIG. 10. Dependence of the parameter σ on the number of randomly chosen chains in a mixture. The number of components n is always increased by adding a chain made by a walk of a greater length. The dashed line represents the logarithmic fit of the form $\sigma = A \ln(kn)$, with $A = 4.76 \pm 0.04$ and $k = 1.41 \pm 0.05$. The statistical error bars do not exceed the size of the symbols.

in the deposition process of a mixture have been studied. We have performed a detailed analysis of the contribution to the densification kinetics coming from each mixture component. Approach to the jamming limit in the case of mixtures is found to be exponential of the form (1). Components also reach their contribution to the jamming limit exponentially with characteristic relaxation time σ that depends on the symmetry properties and size of the objects. Both the partial jamming coverages and the corresponding relaxation times σ decrease very rapidly with the size of the objects making the mixture. Hence, the asymptotic behavior of the coverage, reaching eventually the jamming limit, is dominated by the small particles. For the mixtures of lattice objects of different rotational symmetries but of the same number of segments the relaxation time σ is smaller for more symmetric components in the mixture.

Special attention is paid to the dependence of the densification kinetics on the number of components n in the mixture. We have analyzed the polydisperse mixtures in which the size of shapes making the mixture gradually increases with n. A strong dependence of the jamming limit θ_{jam} of n-component mixtures on the shape of the adsorbed species is obtained. We showed that for the mixtures of more symmetric shapes, such as line segments and triangles, jamming coverage increases with n, contrary to the mixture of less compact (angled) shapes where jamming coverage decreases. It has been shown that the relaxation time σ is linearly related to the number of components in the mixture. The slope of σ vs n lines decreases with the increase of the order of rotational symmetry of the basic shape making the mixture.

We have also presented the numerical results of RSA for mixtures of arbitrarily chosen self-avoiding random walk chains on a square lattice. It is found that the total jamming coverage decreases exponentially with the length of chains making the mixture. We have observed a slow (logarithmic) growth of the relaxation time σ with the number of randomly chosen components making a polydisperse mixture.

Recently, we have performed extensive numerical simulations of the reversible RSA using binary mixtures composed of the shapes of different number of segments and rotational symmetries on a triangular lattice [32]. The presented numerical analysis could be a first step toward dealing with more complex situations, such as the case of reversible adsorption of polydisperse mixtures of extended objects onto 2D lattices.

[1] J. W. Evans, Rev. Mod. Phys. **65**, 1281 (1993).

[2] V. Privman, Colloids Surf., A **165**, 231 (2000).

[3] B. Senger, J. C. Voegel, and P. Schaaf, Colloids Surf., A **165**, 255 (2000).

[4] A. Cadilhe, N. A. M. Araújo, and V. Privman, J. Phys.: Condens. Matter **19**, 065124 (2007).

[5] J. J. González, P. C. Hemmer, and J. S. Høye, Chem. Phys. **3**, 228 (1974).

[6] M. C. Bartelt and V. Privman, Phys. Rev. A **44**, R2227 (1991).

[7] E. Ben-Naim and P. L. Krapivsky, J. Phys. A **27**, 3575 (1994).

[8] Y. Fan and J. K. Percus, J. Stat. Phys. **66**, 263 (1992).

[9] A. Baram and D. Kutasov, J. Phys. A **27**, 3683 (1994).

[10] S. S. Manna and N. M. Švrakić, J. Phys. A **24**, L671 (1991).

[11] Lj. Budinski-Petković and U. Kozmidis-Luburić, Phys. Rev. E **56**, 6904 (1997).

[12] J. W. Lee, Colloids Surf., A **165**, 363 (2000).

[13] V. Cornette, D. Linares, A. J. Ramirez-Pastor, and F. Nieto, J. Phys. A **40**, 11765 (2007).

[14] I. Lončarević, Lj. Budinski-Petković, and S. B. Vrhovac, Eur. Phys. J. E **24**, 19 (2007).

[15] R. Erban and S. J. Chapman, J. Stat. Phys. **127**, 1255 (2007).

[16] J. Feder, J. Theor. Biol. **87**, 237 (1980).

[17] R. H. Swendsen, Phys. Rev. A **24**, 504 (1981).

[18] Y. Pomeau, J. Phys. A **13**, L193 (1980).

[19] B. Bonnier, Phys. Rev. E **64**, 066111 (2001).

[20] M. C. Bartelt and V. Privman, J. Chem. Phys. **93**, 6820 (1990).

[21] P. Nielaba, V. Privman, and J. S. Wang, J. Phys. A **23**, L1187 (1990).

[22] Lj. Budinski-Petković and U. Kozmidis-Luburić, Physica A **236**, 211 (1997).

[23] G. C. Barker and M. J. Grimson, Mol. Phys. **63**, 145 (1988).

[24] P. Meakin and R. Jullien, Phys. Rev. A **46**, 2029 (1992).

[25] B. Bonnier, Y. Leroyer, and E. Pommiers, J. Phys. I **2**, 379 (1992).

[26] Z. Adamczyk, B. Siwek, M. Zembala, and P. Weroński, J. Colloid Interface Sci. **185**, 236 (1997).

[27] N. V. Brilliantov, Y. A. Andrienko, P. L. Krapivsky, and J. Kurths, Phys. Rev. Lett. **76**, 4058 (1996).

[28] N. M. Švrakić and M. Hankel, J. Phys. I **1**, 791 (1991).

[29] J. Talbot and P. Schaaf, Phys. Rev. A **40**, 422 (1989).

[30] G. Tarjus and J. Talbot, Phys. Rev. A **45**, 4162 (1992).

[31] P. L. Krapivsky, J. Stat. Phys. **69**, 135 (1992).

[32] I. Lončarević, Lj. Budinski-Petković, and S. B. Vrhovac, Phys. Rev. E **76**, 031104 (2007).